Correspondence to:

S. Y. Nikiforov,
nikiforov@np.cosmos.ru

Water and Chlorine in the Martian Subsurface Along the Traverse of NASA's Curiosity Rover: 1. DAN Measurement Profiles Along the Traverse

I. G. Mitrofanov[1], S. Y. Nikiforov[1], M. V. Djachkova[1], D. I. Lisov[1], M. L. Litvak[1], A. B. Sanin[1], and A. R. Vasavada[2]

[1]Space Research Institute of the Russian Academy of Sciences (IKI), Moscow, Russia, [2]Jet Propulsion Laboratory, California Institute of Technology, Pasadena, CA, USA

Abstract This paper presents estimates of the water and chlorine contents in the subsurface of Gale crater based on the measurements by the Dynamic Albedo of Neutrons (DAN) instrument onboard the NASA Curiosity rover. It is Part 1 of a two-paper series. Data derived both from DAN active and passive measurements are presented in discrete surface areas (pixels) assuming a homogeneous distribution of water within the DAN sensing depth (60 cm) along the traverse of the rover. It is shown that the content of hydrogen, reported as Water Equivalent Hydrogen, varies between almost zero and a maximum of (6.1 ± 0.7) wt.%. The content of absorption equivalent chlorine varies between almost zero and (2.6 ± 0.2) wt.%. Such variations are thought to be related to the different geological processes and environmental conditions present in the strata along the traverse during the evolutionary history of Gale crater. The second paper (Part 2) studies particular properties of water and abundances of neutron absorbing elements at distinct geological regions, that the rover crossed on its way.

Plain Language Summary The Dynamic Albedo of Neutrons (DAN) is a neutron spectrometer that searches for signs of water by measuring the content of neutron absorbing elements in the ground below the NASA's Curiosity rover. Data derived from DAN are presented in discrete pixels along the traverse of the rover. Each pixel contains estimations of water equivalent hydrogen (WEH) and absorption equivalent chlorine (AEC) content from neutron sensing. DAN observations were combined into the two types of 3×3 m pixels: Pixel with Active Data includes WEH and AEC content and Pixel of Passive Data includes WEH content. Each pixel has been assigned to the associated geological member of the Mars Science Laboratory stratigraphic column. Full DAN data volume for 27 km of the traverse were formatted as a table with more than 10,000 pixels. The large fraction of stratigraphic members (Bradbury, Pahrump Hills and others) have the mean WEH values between 2 and 3 wt.%, while other members of the second part of the traverse (Jura, Knockfarrill Hill, Glasgow, Pontours) have the mean values of WEH above 3 wt.%. Mean AEC value has no large variations for all tested stratigraphic members; it is equal to around 1 wt.% for the majority of the pixels.

1. Introduction

A lot of new knowledge has been provided about the Martian surface by nuclear scientific instruments both on the surface of the planet and onboard orbiting spacecraft (Boynton et al., 2002, 2004; Feldman et al., 2002, 2011; Litvak et al., 2006, 2014, 2016, 2020; Maurice et al., 2011; Mitrofanov et al., 2002, 2003, 2004, 2016, 2018, 2022; Sanin et al., 2017). New results of the neutron spectrometer FREND onboard European Space Agency Trace Gas Orbiter in Valles Marineris area on Mars can be highlighted, where nuclear method revealed permafrost oasis as described in Malakhov et al. (2020) and newly published paper Mitrofanov et al. (2022). The water content in the subsurface of modern Mars characterizes the hydrological evolution of the planet and the processes of interaction between the surface and the atmosphere in the modern era (Bibring et al., 2006). There are regions of particular interest on Mars for detailed measurements of the chemical composition of subsurface, such as those thought to be formed during the epoch of "wet Mars" and therefore are of high interest as potentially habitable environments (Abramov & Kring, 2005).

Curiosity rover is a part of NASA's Mars Exploration Program. The purpose of the mission is to search for past and present habitable environments and study the evolution of the Martian climate (Grotzinger et al., 2012, 2015; Vasavada, 2022). The near-equatorial Gale crater was selected as the research area of Curiosity rover. In situ

investigations have revealed that the lower portions of the crater's interior mound formed within long-lived lakes (Edgar et al., 2020; Rampe et al., 2020). The mission includes the Russian science instrument "Dynamic Albedo of Neutrons" (DAN) (Mitrofanov et al., 2012), which is an active and passive neutron spectrometer. This instrument tracks the abundance of water molecules and chlorine in the shallow subsurface along the rover traverse. The DAN experiment is based on the physical method of neutron activation analysis (Litvak et al., 2008; Mitrofanov et al., 2012). In the active mode of DAN operations, the studied subsurface is irradiated by pulses of high-energy neutrons. The contents of hydrogen and other neutron absorbers (mostly Cl) are determined by analyzing time profiles of post-pulse emission of thermal and epithermal neutrons. In text we will use two parameters: water equivalent of hydrogen (WEH) and absorption equivalent chlorine (AEC), representing the content of hydrogen and the content of other neutron absorbing elements, respectively. Recent studies done by the DAN team have demonstrated that changes in Fe can also result in significant changes in DAN neutron die away data (Czarnecki et al., 2020; Lisov et al., 2018; Mitrofanov et al., 2012). DAN may also be used in the passive mode (Jun et al., 2013; Mitrofanov et al., 2012), when detected neutrons either are produced in the Martian atmosphere and subsurface under the bombardment of high energy particles of Galactic Cosmic Rays (GCR) or are emitted by the rover's Multi-Mission Radioisotope Thermoelectric Generator (MMRTG) and back-scattered in the subsurface.

This paper is the Part 1 of two-paper series. It presents the derivation of a pixelated map of water and AEC values (as a proxy for neutron absorption cross section) within the Martian subsurface, as derived from both active and passive measurements by DAN. This study is the continuation of the previous investigations (Djachkova et al., 2022; Lisov et al., 2018; Mitrofanov et al., 2016; Nikiforov et al., 2020). It is based on measurements performed by DAN during almost 9 years of operations on the Martian surface from August 2012 to December 2021, and represents the pixelated data along the traverse. The Part 2 of two-paper series is devoted to the studies of WEH and AEC abundances within the distinct geological regions, crossed by the rover on its way.

The Curiosity mission is ongoing, and DAN measurements continue to be acquired along the drive path of the rover. The neutron generator DAN pulsed neutron generator (PNG) guaranteed the emission of 10 million neutron pulses. For the current moment it has produced more than 16 million neutron pulses and repeatedly exceeded its technical resource. Generator continues to function nominally on the Martian surface.

2. DAN Active Measurements

The DAN instrument consists of two separate units: detector and electronics block DAN DE and pulsed neutron generator DAN PNG (see Mitrofanov et al., 2012 for details). DAN DE contains two proportional counters filled with ^{3}He gas for recording thermal and epithermal neutrons up to the energy of 100 eV (counter of total neutrons (CTN) detector) and epithermal neutrons from 0.4 eV up to 100 eV (counter of epithermal neutrons (CETN) detector). When DAN DE operates in passive mode, its detectors record the local neutron background. The local neutron background has two components: neutrons that are generated in the Martian subsurface due to the direct bombardment by Galactic Cosmic Rays (GCRs) and those generated by the MMRTG, of which some neutrons propagate directly to the counters while others back-scatter in the shallow subsurface before detection. In the active mode DAN PNG generates short pulses of 14 MeV neutrons, and DAN DE records additional counts of post-pulse emission of moderated neutrons after their interactions with nuclei of shallow subsurface.

Time profiles of post-pulse emission of epithermal and thermal neutrons are determined by the processes of their moderation and absorption in the matter of subsurface. Generally speaking, the fraction of energy lost by a neutron in each scattering on a nucleus is larger when the mass of the nucleus encountered is smaller. Addition of even small amount of hydrogen leads to a rather strong increase of efficiency of neutron moderation: correspondingly, the radiated flux of epithermal neutrons decreases and the flux of thermal neutrons increases. However, there is no conservation law of neutrons in epithermal and thermal energy ranges, because thermal particles could be absorbed by nuclei with large thermal-neutron cross-section, and hydrogen is one among them. Therefore, in addition to estimation of the content of WEH, the data on the dynamic neutron albedo make it possible to estimate the number of nuclei with a large absorption cross section for thermal neutrons. The presence of these nuclei has little effect on the flux of epithermal neutrons, but can significantly reduce the radiation of thermal particles.

For a particular testing spot on the surface, the post-pulse emission is measured during sessions of PNG pulsing activity. Counts of CTN and CETN are distributed in 64 linear time bins corresponding to the neutron time

Table 1
The Content of the Main Regolith-Forming Elements (%) Derived From APXS PDS Data

Elements	O	Si	Fe	Ca	Al	Mg	S	Na	K	Ti	P	Mn	Cr	Total
Average APXS mass fraction (%)	43.3	21.7	13.0	4.8	4.7	4.2	2.7	2.0	0.7	0.6	0.4	0.3	0.2	98.6%
Fractions used for modeling of regolith (%)	43.9	21.9	13.3	4.8	4.7	4.3	2.8	2.0	0.8	0.6	0.4	0.3	0.2	100.0%

profiles from the beginning of each pulse. The time profiles of dynamic albedo of epithermal and thermal + epithermal neutrons are derived from these two recorded time profiles by subtraction of counts of local background, as measured by DAN DE in the passive mode at the same spot just before and after the pulsing session. The data of dynamic albedo for epithermal and thermal neutrons provide estimations of two parameters: hydrogen estimated as WEH and the total contribution of other neutron absorbers estimated as AEC. The estimates showed that chlorine is the main, but not the only, absorber of neutrons in the Martian subsurface (see Hardgrove et al., 2011; Lisov et al., 2018; Mitrofanov et al., 2014; Sanin et al., 2015). The parameter of AEC was suggested for representing the totality of neutron absorbing elements.

This method is based on numerical simulations of neutron scattering in the subsurface. The subsurface composition has variable mass fractions for regolith ξ_R, for WEH ξ_{WEH} and for AEC ξ_{AEC} with $\xi_R + \xi_{WEH} + \xi_{AEC} = 100\%$. The regolith composition is fixed and uses the average (AV) element mass fractions measured by the rover's Alpha Particle X-Ray Spectrometer (APXS, Gellert & Clark, 2015) up to sol 1330 (Table 1). For the model it was scaled in second row according to the element weights on the first row. The value of ξ_{AEC} includes not only chemical Cl, but other neutron absorbers. It differs from the actual chlorine content to compensate the differences between actual and fixed regolith content of neutron absorbers other than H, most importantly Cl and Fe (Lisov et al., 2018; Mitrofanov et al., 2014; Sanin et al., 2015).

The analysis of time profiles of post-pulse emission of thermal and epithermal neutron makes it possible to determine both the values ξ_{WEH} and ξ_{AEC} for the subsurface matter (Lisov et al., 2018; Mitrofanov et al., 2016). Their values can be derived from DAN active data by the comparison between the recorded post-pulse time profiles in CTN and CETN counters and numerically predicted post-pulse time profiles of similar counts in accordance with the testing models of subsurface structure and composition. Two kinds of testing models can be considered. The first one is the homogeneous model of subsurface (HMS). It corresponds to the homogeneous composition of all three components ξ_R, ξ_{WEH}, and ξ_{AEC} in-depth (see Sanin et al., 2015). Obviously, HMS has two free parameters, ξ_{WEH} and ξ_{AEC}. The second testing model is more complex. It assumes that subsurface has two layers with different fractions ξ_{WEH} of WEH. It is named the double-layer model (DLM) as described in Lisov et al., 2018. DLM has four free parameters: $\xi_{WEH}^{(top)}$ for top layer, $\xi_{WEH}^{(bottom)}$ for bottom layer, the depth H of boundary between layers and the single value ξ_{AEC} for AEC in both layers.

The best fitting values for fitting parameters of HMS and DLM are derived using the Pearson's chi-squared test, and they are considered to be the experimental estimates for the fractions of WEH and AEC. The high efficiency of these methods for measuring the WEH content in subsurface has been shown by the previous studies (Lisov et al., 2018; Sanin et al., 2015). For each spot of active DAN measurements, the HMS model is tested for consistency with observations. HMS is accepted in case p-value in Pearson criteria is higher than 1%, otherwise it is rejected. The best fitting values for ξ_{WEH} and ξ_{AEC} are used in this case, as the measured mass fractions for WEH and AEC. If HMS is rejected, the more complex model DLM can be used for fitting the observed post-pulse time profiles at CTN and CETN. However, with the HMS acceptance threshold of 1%, only a fraction of all tested spots, 22% of them, is inconsistent with the HMS. Accordingly, we have decided to accept the simpler HMS model instead of more complex one considering it is supported by observations to cover larger part of the rover traverse. Such an approach allows for a comparison of estimations of WEH and AEC at different areas along the traverse, as they are derived with the same model of the subsurface. Locations inconsistent with HMS are subject of future and more detailed study, such as conducted at individual study sites using more complicated two-layer models or even different subsurface geometries (Gabriel et al., 2017). Further details on the procedure of active data analysis are available in Lisov et al. (2018).

For the period of DAN observations from 9 August 2012 to 21 December 2021, the total path traversed by Curiosity is 27,150 m long; the total number of 1002 active measurements were carried out along this path. The flight

rules of Curiosity permits performing DAN active measurements at the rover stops only, so each DAN active measurement corresponds to an individual tested spot on the surface along the traverse.

The active data analysis has shown that a dominant fraction of spots, namely 78% and 56%, are consistent with the HMS model at the acceptance levels of 1% and 10%, respectively. The basic idea for selection of the minimal grid spacing is the criteria that uncertainty resulted from interpolation between two grid points is smaller than the best-fit uncertainty due to statistical fluctuations of observed counts. Correspondingly, using the threshold of 1% for acceptance of HMS, only a fraction of all tested spots, 22% of them, are inconsistent with the HMS. Therefore, such spots with non-HMS modeling of the subsurface are considered to be exceptional cases. They are not representative of the majority of tested spots along the traverse of the rover.

The main objective of this study is to determine the basic distributions of ξ_{WEH} and ξ_{AEC} for WEH and AEC along the traverse of the rover. They could be derived from the data analysis for the majority of tested spots, which are consistent with HMS. These data of DAN active measurements are used for creation of a pixel-based database for ξ_{WEH} and ξ_{AEC} in Gale crater described below. The spots with non-HMS structure of subsurface should be considered as the unusual phenomena (e.g., as it was identified at Marias Pass by Czarnecki et al., 2020), that needs an individual analysis for each particular case. The reasons of the exceptional uniqueness of these spots will be studied elsewhere in future with the usage of all the data available from the rover scientific instruments.

3. DAN Passive Measurements

As it was mentioned above, the sessions of active measurements were carried out only at rover stops, either shortly after the stop or just before the start of a drive. The spatial resolution of the active neutron sensing is about 3 m around flat terrain (Sanin et al., 2015). Therefore, spots with active measurements can be several tens of meters apart, and only about 11% of the length of Curiosity traverse is covered by such data. Therefore, using the DAN active data, it is possible to build the sampling distributions for values of ξ_{WEH} and ξ_{AEC} for tested spots over the Gale surface, but the sparse sampling makes it difficult to correlate measurements with observed changes in the lithology or surface composition along the traverse. Indeed, active measurements for special research campaigns in some particular areas have shown that local changes of WEH and AEC in the subsurface occur at meter scales (Czarnecki et al., 2020; Gabriel et al., 2018; Litvak et al., 2014, 2016, 2016). Therefore, the possibility of continuous measurements of the WEH content along the rover route is of considerable interest.

Such data can be obtained from DAN operations in the passive mode, when PNG does not emit. DAN DE operates almost continuously and simultaneously with other scientific instruments aboard the rover. It records time profiles of counts of local neutron background in CTN and CETN detectors, with a resolution of 20 s. The "Method of Referencing by Active Data" (MRAD) was suggested by Nikiforov et al., 2020 to derive time profile of WEH content in the shallow subsurface from DAN passive measurements. This method uses the F_{DAN} parameter:

$$F_{DAN} = C_{CTN} / C_{CETN}, \tag{1}$$

where C_{CTN} is the counting rate of the thermal + epithermal neutrons by CTN detector, C_{CETN} is the counting rate of the epithermal neutrons by CETN detector. The usage of such a dimensionless parameter allows us to exclude the effects of neutron counts changing due to variations of GCR flux, and changes of distance from the MMRTG to the surface. This parameter was described in Nikiforov et al. (2020) and these effects are included in the parameter uncertainty. Those samples for which both active and passive measurements were carried out and for which active measurements were consistent with HMS were selected for implementing the MRAD method. The totality of derived values ξ_{WEH} and ξ_{AEC} for such samples were divided into 10 groups corresponding to 10 intervals $[\xi_{AEC}]$ as was described in Nikiforov et al. (2020). In each group, an empirical relationship was drawn up between the values of ξ_{WEH}, as derived from active data, and the values of F_{DAN}, as estimated from the passive data at the same tested spots. A good correlation (≥ 0.75) between ξ_{WEH} and F_{DAN} was found for each group (Nikiforov et al., 2020).

Therefore, the MRAD method allows deriving the value of WEH from the value of F_{DAN} for selected distance interval, provided that the value ξ_{AEC} is known. Usually this value is taken, as derived from active data at the nearest tested spots, or linear interpolated between two nearest spots (see Nikiforov et al., 2020). The value of
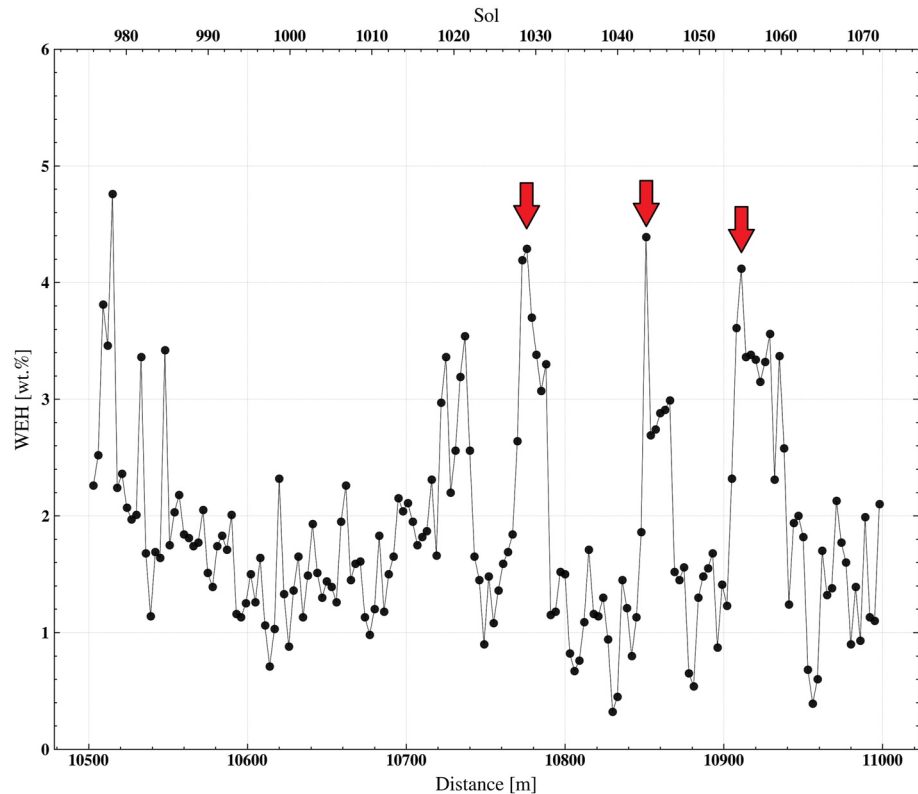
Figure 1. Profile of the spatial variability of the hydrogen content WEH, as derived from DAN passive measurements in the subsurface with a spatial resolution of 3 m. Arrows point to the spots with increased WEH. Section of the traverse is shown for the sols interval 976–1072.

WEH mass fraction, as derived from DAN passive measurements, is defined as ζ_{WEH} to be distinguishable from DAN active measurements.

Figure 1 presents an example of WEH variation profile along a distance interval from 10,500 to 11,000 m (sols 976–1072) with a spatial resolution of 3 m. Note that the distance is measured along the path of the rover and is not necessarily a straight-line distance. One sees 3 distinct peaks of WEH at distance marks of 10,780, 10,860, and 10,920 m (denoted by arrows). However, the shape of the actual path of the rover in this area shows that these peaks do not correspond to different spots on the surface, but are associated with a single water-enriched spot, that was crossed 3 times (see Section 4 below). Therefore, certain difficulties arise for interpretation of such profiles when the rover makes complex motions with multiple crossings of the same point or with several U-turns. This example shows that the profile of WEH versus rover distance does not necessarily represent the actual spatial variations of WEH in the subsurface. The most appropriate approach to represent such variations is suggested in the next section.

4. Presentation of DAN Data as Individual Pixels

The presentation of DAN data as individual pixels is proposed in order to analyze DAN measurements along a complex drive path of the rover in correspondence with the features of local geology, the sides of pixels are oriented in the latitudinal-longitudinal directions. The values of WEH and AEC for the different spots along the rover traverse located within a pixel are averaged and assigned to this pixel. The pixel size was chosen according to the spatial resolution of active measurements, the irradiated area of which has a diameter of 3 m (Sanin et al., 2015). Thus, a 3 × 3 m pixel makes it possible to cover individual active measurements. This choice of pixel size is a compromise between better precision of the results and pixel area coverage. Figure 2 presents the same segment of the traverse as showed in Figure 1 in pixels. There are three clearly visible peaks in the profile at 10,780, 10,860, and 10,920 m (Figure 1), that are associated with the same spot on the surface, shown with a
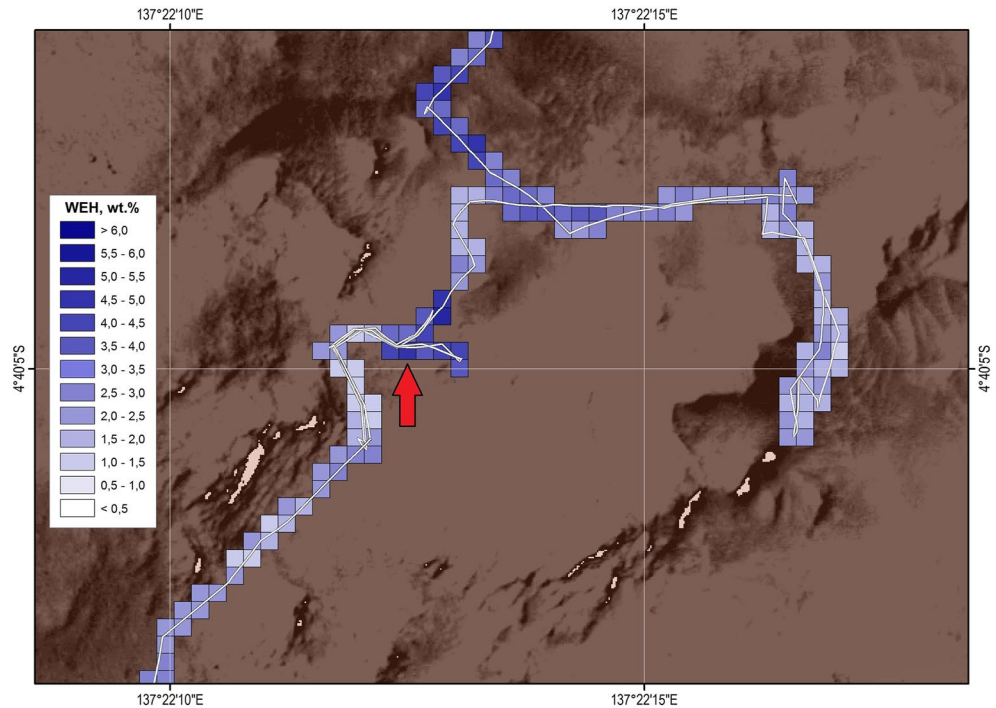
Figure 2. A 3 × 3 meter pixel representation of WEH estimations. Red arrow points to the same area with high WEH values as in Figure 1. The white line is the traverse of the Curiosity rover's center.

red arrow (Figure 2). In order to take into account such complexity of the traverse path, it is proposed to present the DAN data in the form of pixels covering the surface along the path.

For the total traversed path of Curiosity with the length of 27,100 m there are 10,061 pixels. Generally, pixels have successive numbers along the traverse. But there are some cases, when the sequence of numbers is broken: it takes place when the rover makes complex path in some particular areas (see Figure 2 as an example). In such cases, the numbering goes from up to down and from left to right.

The traverse of the rover crosses several geological regions that have been identified using the data available from Curiosity and other missions. The primary way of organizing the observed geology (primarily lithology) used by the mission science team is through the generation of a stratigraphic column (e.g., Rampe et al., 2020), divided into informal groups, formations, and members, with different lithologies derived from rover observations by elevation (Figure 3). Each DAN pixel has been assigned to a particular member. When a pixel crosses a member boundary, it is associated with the member that contains the larger fraction of the pixel's area. The association of DAN pixels with the stratigraphic column divisions is intended for future analyses and correlations with other observed surface characteristics.

The results of active and passive DAN measurements along the traverse are assigned to two independent types of pixels.

748 pixels contains tested spots by DAN active measurements, that are consistent with HMS of subsurface. These pixels are named PADs (Pixels of Active Data). They constitute 7% of the total number of pixels covering the rover path.

There are 93% of pixels along the traverse, the surfaces of which have not been tested by active measurements. One needs to use the DAN passive data to characterize them. They are named PPDs (Pixels of Passive Data). To estimate PPD WEH content from the passively measured parameters of F_{DAN} it is necessary to know the AEC value in current location. Figures 4 and 5 represent distributions of WEH values in PADs and PPDs, and ξ_{AEC} for the entire totality of PADs.
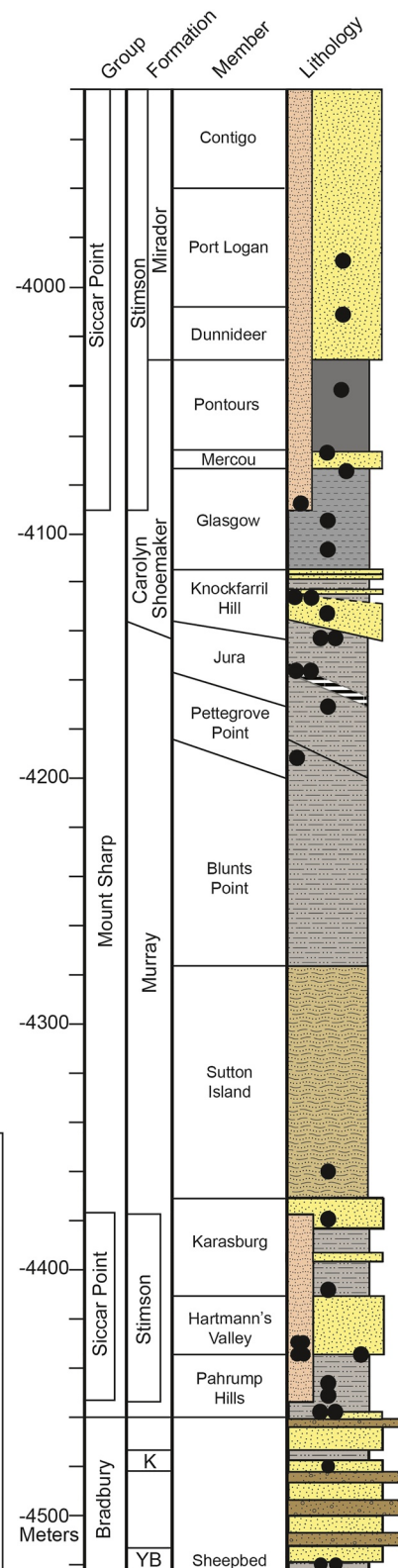
Figure 3. Stratigraphic column for the sedimentary units investigated along Curiosity's traverse. The major groups include Bradbury (investigated along the crater floor), Mount Sharp (the through-going strata of the crater's central mound), and Siccar Point (strata that truncate and unconformably overlie the Mount Sharp group). DAN pixels are associated with stratigraphy at the member level (Fedo et al., 2022; Gwizd et al., 2022).
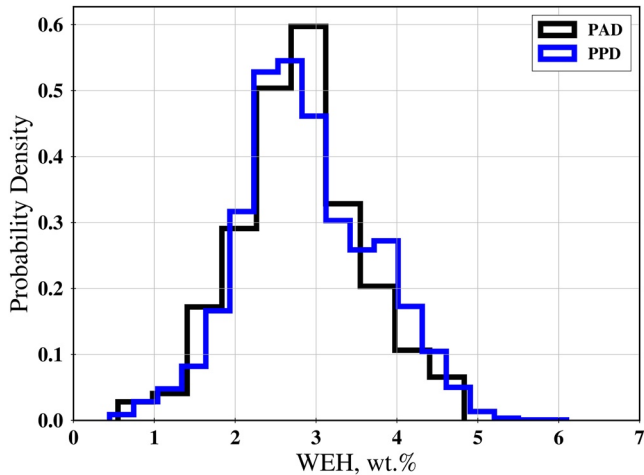
Figure 4. Distribution of the pixel-averaged values of WEH derived from active (black line) and passive (blue line) DAN measurements. Both distributions areas are normalized to 1.

The following approach of solving the problem of the unknown value of ξ_{AEC} was suggested. The distribution of ξ_{AEC} values might be composed for each geological member (see Figure 3) based on the PAD's values in this member. The large number of values of ξ_{AEC} are randomly simulated for each PPD for this member using such distribution. Correspondingly, the large number of ζ_{WEH} values are derived, based on simulated values of ξ_{AEC} and the mean value of F_{DAN} for this pixel. The mean and the sample variance of simulated values of ζ_{WEH} are calculated. They are considered as the derived value of ζ_{WEH} and its uncertainty for such PPD. Figure 4 shows the distribution of derived WEH values by active (ξ_{WEH}) and passive (ζ_{WEH}) estimations. This distribution of ζ_{WEH} is broader than the one for the values of ξ_{WEH} as it represents the continuous sequence of PPD pixels in comparison with ξ_{WEH} values for discrete sub-sequence of pixels PAD located only at the rover stops. Therefore, the uncertainty in WEH between PAD locations is substantially greater than the WEH derived from PAD locations.

The knowledge of ζ_{WEH} for the sequence of PPD pixels provides the continuous distance profile of WEH variations with the spatial resolution of 3 m (see Figure 6 as an example). The sequence of PADs along the Curiosity traverse is shown in Figure 6. For each pixel the value of ξ_{WEH} is shown by different brightness of blue and color scale is identical for both types of pixels. The traverse distance is 600 m for period from sol 1781 to sol 1848. The pixels of active measurements are shown in circles with white outline. The mean distance between successive active pixels is 30 m. The passive WEH estimations are almost continuous and are shown in successive squares with thin black outline. Two types of pixels need to be considered for the spatial WEH profile.

The entire totality of 10,061 pixels, both PADs and PPDs, are presented in the Table 2 of DAN Pixelization Data in Nikiforov et al., 2022, data set. The Table 2 contains in columns: (a) is the successive number of pixel, (b) is a mark of its type, either PAD or PPD, (c) is longitude and (d) is latitude coordinates of the center of the pixel, (e) is the associated member of the stratigraphic column, and (f) is estimated WEH values (ξ_{WEH} for PAD and ζ_{WEH} for PPD, wt.%) and (g) is AEC values ξ_{AEC} for PAD (wt.%). Table 2 presents several lines as example. These lines correspond to pixels PAD or PPD with the maxima of WEH (see Conclusions below).

Members of stratigraphic column differ by WEH and AEC mean values. The large fraction of stratigraphic members have the mean WEH values between 2 and 3 wt.%; they are Bradbury, Sheepbed, Pahrump Hills, Hartmann's Valley, Karasburg, Sutton Island, Blunts Point, Pettegrove Point and Mont Mercou. On the other hand, there are few members at the second part of traverse, namely Jura, Knockfarrill Hill, Glasgow, Pontours, that have the mean values of WEH above 3 wt.%. There are no large variations of mean AEC for all tested stratigraphic members; they all are around 1 wt.%.
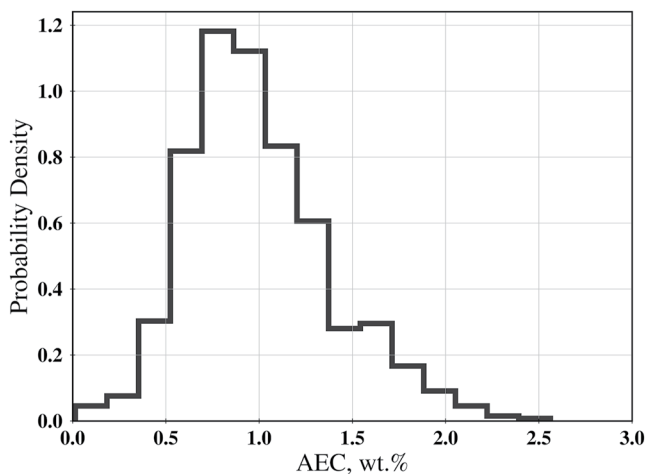
In the second paper of this series, the Part 2, the PAD and PPD are used to study the individual properties of WEH and AEC for each geologic member in more detail.

5. Conclusions

It is the Part 1 of two-paper series. This paper provides profiles of DAN measurements represented as regularly sized pixels along the rover's 27-km traverse. Each pixel contains an estimate of the content of the water equivalent hydrogen (WEH) and the absorption equivalent chlorine (AEC) derived from DAN data collected from 9 August 2012 to 21 December 2021 (sol 3333). DAN measurements are further associated with distinct geological
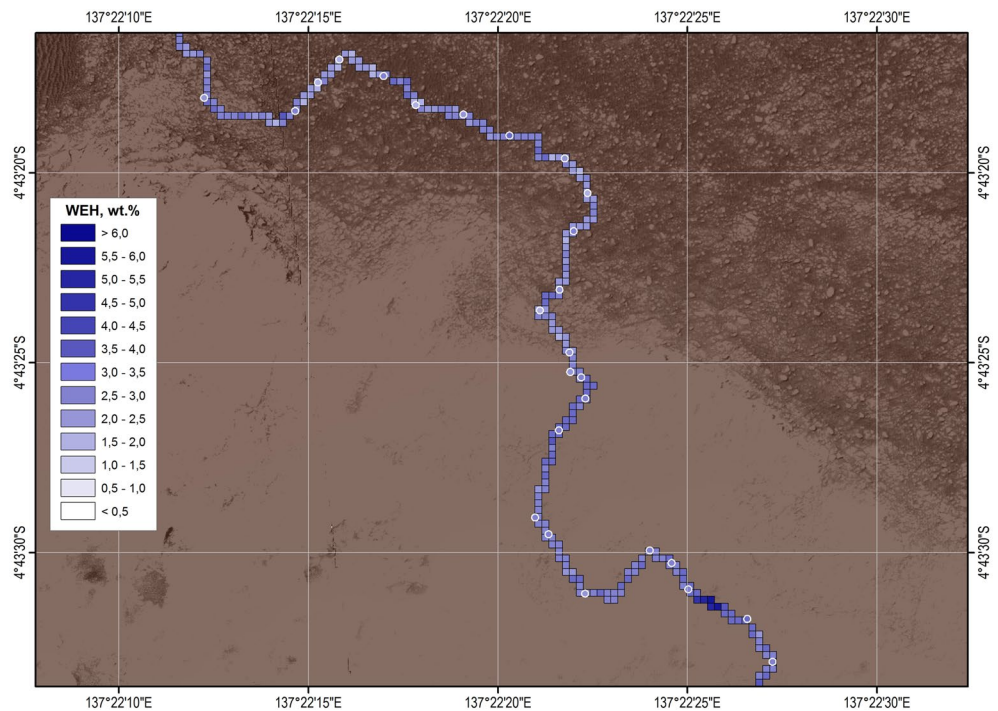

Figure 5. Distribution of the pixel-averaged values ξ_{AEC} derived from the active DAN measurements. Distribution area is normalized to 1.

Figure 6. The sequence of 243 PPD (squares) and 27 PAD (circles) pixels along the Curiosity traverse in time period from sol 1781 to sol 1848.

units along the traverse. Pixel representation has the advantage over previously published DAN results (Nikiforov et al., 2020) of solving the spatial referencing problem for complex rover paths.

The maximum of WEH (6.1 ± 0.7) wt.% is observed in the passive data, PPD ID 6106 in Sutton Island member of Murray formation. It is much larger than the maximum of WEH, as observed in the active data, PAD ID 8704.1 in Knockfarrill Hill member of Carolyn Shoemaker formation. Parameters of these particular pixels are shown in the Table 2, as examples. The content of chlorine varies between almost zero and the highest value in accordance with active measurements. The maximum of AEC (2.56 ± 0.21) wt.% is observed in the active data, PAD ID 2376.1 in Bradbury group.

This full DAN data volume and the map of the whole traverse up to sol 3333 are formatted as the data set Nikiforov et al. (2022).

The measured WEH and AEC variations are hypothesized to be related to the different processes of deposition and diagenesis in the distinct associated geological members of the stratigraphic column (see Figure 3). A second

Table 2
DAN Pixelization Data

Pixel ID	Pixel type	Longitude (center of pixel)	Latitude (center of pixel)	Associated member of the stratigraphic column	WEH values (wt.%)	AEC values (wt.%)
(1)	(2)	(3)	(4)	(5)	(6)	(7)
…	…	…	…	…	…	…
6106	PPD	137.36097	−4.71608	Murray/Sutton Island	6.1 ± 0.7	-
…	…	…	…	…	…	…
8704	PPD	137.39154	−4.73010	Carolyn Shoemaker/Knockfarrill Hill	4.62 ± 0.58	-
8704.1	PAD	137.39154	−4.73010	Carolyn Shoemaker/Knockfarrill Hill	4.83 ± 0.27	1.07 ± 0.14
…	…	…	…	…	…	…

paper in this work studies particular properties of WEH and AEC abundances in particular members examined by the rover.

The Curiosity mission is ongoing, and DAN measurements continue to be acquired along the drive path of the rover. Presented work will be also continued in the future as the new data become available.

Data Availability Statement

DAN data are available in NASA's Planetary Data System (PDS) geosciences node (Mitrofanov, 2012). DAN derived data set are available in zenodo.org archive (Nikiforov et al., 2022).

References

Abramov, O., & Kring, D. A. (2005). Impact-induced hydrothermal activity on early Mars. *Journal of Geophysical Research E: Planets*, *110*(12), 1–19. https://doi.org/10.1029/2005JE002453

Bibring, J.-P., Langevin, Y., Mustard, J. F., Poulet, F., Arvidson, R., Gendrin, A., et al. (2006). Global mineralogical and aqueous Mars history derived from OMEGA/Mars express data. *Science*, *312*(5772), 400–404. https://doi.org/10.1126/science.1122659

Boynton, W. V., Feldman, W. C., Squyres, S. W., Prettyman, T. H., Brückner, J., Evans, L. G., et al. (2002). Distribution of hydrogen in the near surface of Mars: Evidence for subsurface ice deposits. *Science*, *297*(5578), 81–85. https://doi.org/10.1126/science.1073722

Boynton, W. V. V., Feldman, W. C. C., Mitrofanov, I. G. G., Evans, L. G. G., Reedy, R. C. C., Squyres, S. W. W., et al. (2004). The Mars odyssey gamma-ray spectrometer instrument suite. *Space Science Reviews*, *110*(1/2), 37–83. https://doi.org/10.1023/B:SPAC.0000021007.76126.15

Czarnecki, S., Hardgrove, C., Gasda, P. J., Gabriel, T. S. J., Starr, M., Rice, M. S., et al. (2020). Identification and description of a silicic volcaniclastic layer in Gale Crater, Mars, using active neutron interrogation. *Journal of Geophysical Research: Planets*, *125*(3), e2019JE006180. https://doi.org/10.1029/2019JE006180

Djachkova, M. V., Mitrofanov, I. G., Nikiforov, S. Y., Lisov, D. I., Litvak, M. L., & Sanin, A. B. (2022). Testing correspondence between areas with hydrated minerals, as observed by CRISM/MRO, and spots of enhanced subsurface water content, as found by DAN along the traverse of curiosity. *Advances in Astronomy*, *2022*, 1–10. https://doi.org/10.1155/2022/6672456

Edgar, L. A., Fedo, C. M., Gupta, S., Banham, S. G., Fraeman, A. A., Grotzinger, J. P., et al. (2020). A lacustrine paleo environment recorded at vera rubin ridge, gale crater: Overview of the Sedimentology and stratigraphy observed by the Mars Science Laboratory curiosity rover. *Journal of Geophysical Research: Planets*, *125*(3), e2019JE006307. https://doi.org/10.1029/2019JE006307

Fedo, C. M., Bryk, A. B., Edgar, L. A., Bennett, K. A., Fox, V. K., Dietrich, W. E., et al. (2022). Geology and stratigraphic correlation of the Murray and Carolyn shoemaker formations across the glen torridon region, gale crater, Mars. *Journal of Geophysical Research: Planets*, *127*(9), e2022JE007408. https://doi.org/10.1029/2022JE007408

Feldman, W. C., Boynton, W. V., Tokar, R. L., Prettyman, T. H., Gasnault, O., Squyres, S. W., et al. (2002). Global distribution of neutrons from Mars: Results from Mars Odyssey. *Science*, *297*(5578), 75–78. https://doi.org/10.1126/science.1073541

Feldman, W. C., Pathare, A., Maurice, S., Prettyman, T. H., Lawrence, D. J., Milliken, R. E., & Travis, B. J. (2011). Mars Odyssey neutron data: 2. Search for buried excess water ice deposits at nonpolar latitudes on Mars. *Journal of Geophysical Research*, *116*(E11), E11009. https://doi.org/10.1029/2011JE003806

Gabriel, T. S. J., Hardgrove, C., Czarnecki, S., Rampe, E. B., Rapin, W., Achilles, C. N., et al. (2018). Water abundance of dunes in gale crater, Mars from active neutron experiments and implications for amorphous phases. *Geophysical Research Letters*, *45*(23), 12766–12775. https://doi.org/10.1029/2018GL079045

Gabriel, T. S. J., Hardgrove, C., Litvak, M. L., Mitrofanov, I. G., Boynton, W., Fedosov, F., & Nikiforov, S. Y. (2017). Bulk hydrogen content of high-silica rocks in gale crater with the active dynamic albedo of neutrons experiment. *Lunar and Planetary Science*, *XLVIII*, 6–7.

Gellert, R., & Clark, B. C. (2015). In situ compositional measurements of rocks and soils with the alpha particle X-ray spectrometer on NASA's Mars rovers. *Elements*, *11*(1), 39–44. https://doi.org/10.2113/gselements.11.1.39

Grotzinger, J. P., Crisp, J., Vasavada, A. R., Anderson, R. C., Baker, C. J., Barry, R., et al. (2012). Mars Science Laboratory mission and science investigation. *Space Science Reviews*, *170*(1–4), 5–56. https://doi.org/10.1007/s11214-012-9892-2

Grotzinger, J. P., Gupta, S., Malin, M. C., Rubin, D. M., Schieber, J., Siebach, K., et al. (2015). Deposition, exhumation, and paleoclimate of an ancient lake deposit, Gale crater, Mars. *Science*, *350*(6257). https://doi.org/10.1126/science.aac7575

Gwizd, S., Fedo, C., Grotzinger, J., Banham, S., Rivera-Hernández, F., Stack, K. M., et al. (2022). Sedimentological and geochemical perspectives on a marginal lake environment recorded in the Hartmann's Valley and Karasburg members of the Murray formation, Gale crater, Mars. *Journal of Geophysical Research: Planets*, *127*(8), e2022JE007280. https://doi.org/10.1029/2022JE007280

Hardgrove, C., Moersch, J., & Drake, D. (2011). Effects of geochemical composition on neutron die-away measurements: Implications for Mars Science Laboratory's dynamic albedo of neutrons experiment. *Nuclear Instruments and Methods in Physics Research Section A: Accelerators, Spectrometers, Detectors and Associated Equipment*, *659*(1), 442–455. https://doi.org/10.1016/j.nima.2011.08.058

Jun, I., Mitrofanov, I., Litvak, M. L., Sanin, A. B., Kim, W., Behar, A., et al. (2013). Neutron background environment measured by the Mars Science Laboratory's dynamic albedo of neutrons instrument during the first 100 sols. *Journal of Geophysical Research: Planets*, *118*(11), 2400–2412. https://doi.org/10.1002/2013JE004510

Lisov, D. I., Litvak, M. L., Kozyrev, A. S., Mitrofanov, I. G., & Sanin, A. B. (2018). Data processing results for the active neutron measurements by the DAN instrument on the curiosity Mars rover. *Astronomy Letters*, *44*(7), 482–489. https://doi.org/10.1134/S1063773718070034

Litvak, M. L., Mitrofanov, I. G., Barmakov, Y. N., Behar, A., Bitulev, A., Bobrovnitsky, Y., et al. (2008). The dynamic albedo of neutrons (DAN) experiment for NASA's 2009 Mars Science Laboratory. *Astrobiology*, *8*(3), 605–612. https://doi.org/10.1089/ast.2007.0157

Litvak, M. L., Mitrofanov, I. G., Hardgrove, C., Stack, K. M., Sanin, A. B., Lisov, D., et al. (2016). Hydrogen and chlorine abundances in the Kimberley formation of Gale crater measured by the DAN instrument on board the Mars Science Laboratory Curiosity rover. *Journal of Geophysical Research: Planets*, *121*(5), 836–845. https://doi.org/10.1002/2015JE004960

Litvak, M. L., Mitrofanov, I. G., Kozyrev, A. S., Sanin, A. B., Tretyakov, V. I., Boynton, W. V., et al. (2006). Comparison between polar regions of Mars from HEND/Odyssey data. *Icarus*, *180*(1), 23–37. https://doi.org/10.1016/j.icarus.2005.08.009

Litvak, M. L., Mitrofanov, I. G., Sanin, A. B., Lisov, D., Behar, A., Boynton, W. V., et al. (2014). Local variations of bulk hydrogen and chlorine-equivalent neutron absorption content measured at the contact between the Sheepbed and Gillespie Lake units in Yellowknife

Bay, Gale Crater, using the DAN instrument onboard Curiosity. *Journal of Geophysical Research: Planets*, *119*(6), 1259–1275. https://doi.org/10.1002/2013JE004556

Litvak, M. L., Sanin, A. B., Mitrofanov, I. G., Bakhtin, B., Jun, I., Martinez-Sierra, L. M., et al. (2020). Mars neutron radiation environment from HEND/Odyssey and DAN/MSL observations. *Planetary and Space Science*, *184*, 104866. https://doi.org/10.1016/j.pss.2020.104866

Malakhov, A. V. V., Mitrofanov, I. G. G., Litvak, M. L. L., Sanin, A. B. B., Golovin, D. V. V., Djachkova, M. V. V., et al. (2020). Ice permafrost "Oases" close to Martian equator: Planet neutron mapping based on data of FREND instrument onboard TGO orbiter of Russian-European ExoMars mission. *Astronomy Letters*, *46*(6), 407–421. https://doi.org/10.1134/S1063773720060079

Maurice, S., Feldman, W., Diez, B., Gasnault, O., Lawrence, D. J., Pathare, A., & Prettyman, T. (2011). Mars Odyssey neutron data: 1. Data processing and models of water-equivalent-hydrogen distribution. *Journal of Geophysical Research*, *116*(E11), E11008. https://doi.org/10.1029/2011JE003810

Mitrofanov, I. (2012). Mars Science Laboratory dynamic albedo of neutrons EDR Data V1.0, MSL-L-DAN-2-EDR-V1.0. *NASA Planetary Data System*. https://doi.org/10.17189/1519455

Mitrofanov, I., Anfimov, D., Kozyrev, A., Litvak, M., Sanin, A., Tret'yakov, V., et al. (2002). Maps of subsurface hydrogen from the high energy neutron detector, Mars Odyssey. *Science*, *297*(5578), 78–81. https://doi.org/10.1126/science.1073616

Mitrofanov, I., Malakhov, A., Bakhtin, B., Golovin, D., Kozyrev, A., Litvak, M., et al. (2018). Fine resolution epithermal neutron detector (FREND) Onboard the ExoMars trace gas orbiter. *Space Science Reviews*, *214*(5), 86. https://doi.org/10.1007/s11214-018-0522-5

Mitrofanov, I., Malakhov, A., Djachkova, M., Golovin, D., Litvak, M., Mokrousov, M., et al. (2022). The evidence for unusually high hydrogen abundances in the central part of Valles Marineris on Mars. *Icarus*, *374*, 114805. https://doi.org/10.1016/j.icarus.2021.114805

Mitrofanov, I. G., Kozyrev, A. S., Lisov, D. I., Vostrukhin, A. A., Golovin, D. V., Litvak, M. L., et al. (2016). Active neutron sensing of the Martian surface with the DAN experiment onboard the NASA "Curiosity" Mars rover: Two types of soil with different water content in the Gale crater. *Astronomy Letters*, *42*(4), 251–259. https://doi.org/10.1134/S1063773716040058

Mitrofanov, I. G., Litvak, M. L., Kozyrev, A. S., Sanin, A. B., Tret'yakov, V. I., Grin'kov, V. Y., et al. (2004). Soil water content on Mars as estimated from neutron measurements by the HEND instrument onboard the 2001 Mars Odyssey spacecraft. *Solar System Research*, *38*(4), 253–257. https://doi.org/10.1023/B:SOLS.0000037461.70809.45

Mitrofanov, I. G., Litvak, M. L., Sanin, A. B., Starr, R. D., Lisov, D. I., Kuzmin, R. O., et al. (2014). Water and chlorine content in the Martian soil along the first 1900 m of the Curiosity rover traverse as estimated by the DAN instrument. *Journal of Geophysical Research: Planets*, *119*(7), 1579–1596. https://doi.org/10.1002/2013JE004553

Mitrofanov, I. G., Litvak, M. L., Varenikov, A. B., Barmakov, Y. N., Behar, A., Bobrovnitsky, Y. I., et al. (2012). Dynamic albedo of neutrons (DAN) experiment onboard NASA's Mars Science Laboratory. *Space Science Reviews*, *170*(1–4), 559–582. https://doi.org/10.1007/s11214-012-9924-y

Mitrofanov, I. G., Zuber, M. T., Litvak, M. L., Boynton, W. V., Smith, D. E., Drake, D., et al. (2003). CO_2 snow depth and subsurface water-ice abundance in the northern hemisphere of Mars. *Science*, *300*(5628), 2081–2084. https://doi.org/10.1126/science.1084350

Nikiforov, S., Djachkova, M., & Lisov, D. (2022). Water and chlorine in the Martian subsurface along the traverse of NASA's curiosity rover: DAN measurement profiles along the traverse (version 1) [Dataset]. Zenodo. https://doi.org/10.5281/zenodo.6974535

Nikiforov, S. Y., Mitrofanov, I. G., Litvak, M. L., Lisov, D. I., Djachkova, M. V., Jun, I., et al. (2020). Assessment of water content in Martian subsurface along the traverse of the Curiosity rover based on passive measurements of the DAN instrument. *Icarus*, *346*, 113818. https://doi.org/10.1016/j.icarus.2020.113818

Rampe, E. B., Blake, D. F., Bristow, T. F., Ming, D. W., Vaniman, D. T., Morris, R. V., et al. (2020). Mineralogy and geochemistry of sedimentary rocks and eolian sediments in Gale crater, Mars: A review after six Earth years of exploration with curiosity. *Geochemistry*, *80*(2), 125605. https://doi.org/10.1016/j.chemer.2020.125605

Sanin, A. B., Mitrofanov, I. G., Litvak, M. L., Bakhtin, B. N., Bodnarik, J. G., Boynton, W. V., et al. (2017). Hydrogen distribution in the lunar polar regions. *Icarus*, *283*, 20–30. https://doi.org/10.1016/j.icarus.2016.06.002

Sanin, A. B., Mitrofanov, I. G., Litvak, M. L., Lisov, D. I., Starr, R., Boynton, W., et al. (2015). Data processing of the active neutron experiment DAN for a Martian regolith investigation. *Nuclear Instruments and Methods in Physics Research Section A: Accelerators, Spectrometers, Detectors and Associated Equipment*, *789*, 114–127. https://doi.org/10.1016/j.nima.2015.03.085

Vasavada, A. R. (2022). Mission overview and scientific contributions from the Mars Science Laboratory curiosity rover after eight years of surface operations. *Space Science Reviews*, *218*(3), 14. https://doi.org/10.1007/s11214-022-00882-7